Available online at www.sciencedirect.com
SCIENCE DIRECT®
Organic Electronics 5 (2004) 107–114
Organic Electronics
www.elsevier.com/locate/orgel

Molecular stacking and emission properties in Langmuir–Blodgett films of two alkyl substituted perylene tetracarboxylic diimides

T. del Caño [a], V. Parra [b], M.L. Rodríguez-Méndez [b], R. Aroca [c], J.A. de Saja [a,*]

[a] *Dpto. Física de la Materia Condensada, Facultad de Ciencias, Universidad de Valladolid, Pº Prado de la Magdelena s/n, 47005 Valladolid, Spain*
[b] *Dpto. Química Inorgánica, E.T.S.I.I, Universidad de Valladolid, Pº Paseo del Cauce s/n, 47011 Valladolid, Spain*
[c] *Materials and Surface Group, School of Physical Sciences, University of Windsor, 4012 Sunset Ave., Windsor, Ont., Canada N9B 3P4*

Received 6 June 2003; received in revised form 27 October 2003; accepted 18 November 2003
Available online 7 December 2003

Abstract

The structural and optical properties of Langmuir–Blodgett (LB) films of two perylene diimide derivates, *N*,*N*′-Bis(propyl)-3,4,9,10-perylenebis(dicarboximide) and *N*,*N*′-Bis(neopentyl)-3,4,9,10-perylenebis(dicarboximide), are reported. The surface pressure–area (π–*A*) isotherms have evidenced how the lateral chain substituents control the strength of the intermolecular interaction. Nevertheless, a head-on tilted molecular orientation on the water subphase was found for both compounds. This molecular orientation is preserved when the monolayers are transferred onto substrates. Molecular orientation in the films was extracted from comparative analysis of transmission and reflection–absorption infrared spectroscopy (RAIRS) data. Film structure has been studied by means of atomic force microscopy (AFM). The observed different emission profiles have been correlated with the ability of the derivatives to get coupled.

Keywords: Organic semiconductors; Perylene diimide derivates; Langmuir–Blodgett films

1. Introduction

Organic semiconductors have emerged in the last decade as main active components in practical thin film devices as photovoltaic cells, light emitting displays and other electronic devices [1–3]. In particular, perylene diimides derivatives have attracted the attention of the scientific community owing to their chemical and thermal stability, electron affinity—enabling n-type semiconductor behaviour—and useful photophysical properties [4–11]. In addition, perylene diimides are vacuum compatible and, in appropriate solvents, suitable for Langmuir–Blodgett technique fabrication [12]. Perylene diimides, being aromatic molecules with extensive π-system and considerable planarity, exhibit a clear tendency to self-alignment. Therefore, the fabrication of ordered thin films can be achieved with these compounds

* Corresponding author. Tel.: +34-983-423196; fax: +34-983-423192.
E-mail address: sajasaez@fmc.uva.es (J.A. de Saja).

1566-1199/$ - see front matter
doi:10.1016/j.orgel.2003.11.004

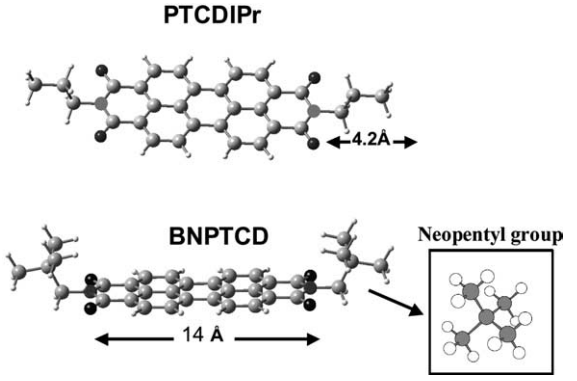

Fig. 1. DFT optimized molecular geometry of BNPTCD and PTCDIPr. (H white, C gray, N dark gray, O black.)

[13,14]. On the other hand, photophysical and electronic properties found in perylene-based thin films are related to the presence of different molecular stacking arrangements [6,15]. Thus, the study of molecular packing provides fundamental information for further understanding of the performance of electronic devices based on these materials.

The objective of this work was to study and compare the optical characteristics of thin films of two perylene diimides which chemical structures differed in the alkyl lateral chain attached to the chromophore (Fig. 1). The Langmuir–Blodgett technique was chosen as fabrication procedure allowing the achievement of ordered films. Molecular organization was elucidated from infrared data obtained in transmission and reflection–absorption modes. Complementary information related to film morphology was extracted by means of AFM topographical analysis.

2. Experimental section

2.1. Materials

N,*N*′-Bis(propyl)-3,4,9,10-perylenebis(dicarboximide) (denoted as PTCDIPr) and *N*,*N*′-Bis(neopentyl)-3,4,9,10-perylenebis(dicarboximide) (denoted as BNPTCD) were kindly provided by Dr. James Duff from the Xerox Research Center of Canada. The synthesis of both materials has been previously reported [8,16]. All chemical and solvents (Aldrich Chemical Ltd.) were of reagent grade and used as supplied.

2.2. Optimized geometry

The molecular structures of BNPTCD and PTCDIPr were optimized with a Gaussian98 suite of programs using the density functional theory (DFT) methodology, and selecting the tight RB3LYP/6-31G basis set.

2.3. Film preparation

Langmuir and Langmuir–Blodgett films were fabricated using a KSV 5000 LB through. BNPTCD and PTCDIPr powders were dissolved in dichloromethane: trifluoroacetic acid (95:5) mixed solvent with initial concentrations 1.1×10^{-4} and 7.5×10^{-5} moll^{-1}, respectively. Solutions were sonicated and, then, spread onto ultra pure water (Millipore, MilliQ). The water bath temperature was kept constant at 20 °C. After evaporation of the solvent, the floating molecules were compressed at a speed of 8 mm/min. The monolayers were then transferred at a speed of 5 mm/min to highly clean quartz, mica and gold substrates at target pressures of 30 and 29 mN/m for PTCDIPr and BNPTCD, respectively. Z-deposition was used to build the LB films of both compounds; the substrate was immersed into the water before spreading the solution and lifted after compressing the monolayer. Several monolayers where successfully transferred. The transfer ratios were near the unity up to the ninth monolayer for BNPTCD and 13th monolayer for PTCDIPr. Further transferring leads to a decrease of the transfer ratios.

2.4. Films characterization

The electronic absorption spectra of solutions and LB films were recorded with a double beam UV–Visible SHIMADZU 2101 spectrometer.

Transmission and RAIRS infrared spectra were recorded using a Nicolet Magna IR 760 spectrometer equipped with a DGTs detector. 1000

scans infrared spectra were recorded using resolution of 2 cm^{-1}. The sample chamber was purged with N_2 for one-hour prior measurements were attended. The RAIRS measurements were recorded at an incident angle of 80°. The gold films (500 Å mass thickness) used as substrates for RAIRS measurements were prepared by high vacuum deposition (BALZERS SCD004). Smooth gold substrates were chosen as reflecting surface since no chemical bonding between the metal surface and the species is expected. Therefore, it can be assumed that the same molecular orientation upheld on other substrates.

Photoluminescence measurements were carried out in a Renishaw Research Raman Microscope System RM2000 equipped with a Leica microscope (DMLM series) using the 514.5 nm argon ion laser line as the excitation source. A 50× microscope objective focuses the laser beam onto a sample spot of ca. 1.0 μm^2 and the emission spectra are recorded using a Peltier cooled (−70 °C) CCD array.

AFM topographical images LB films transferred onto freshly cleaved mica were recorded with a Topometrix TMX 2010 Discoverer instrument in contact mode.

3. Results and discussion

3.1. Surface pressure–area isotherms of Langmuir films

Reproducible surface pressure–area isotherms of the BNPTCD and PTCDIPr Langmuir films were obtained and examples are shown in Fig. 2. The isotherms of both compounds exhibit large stable solid phases. However, differences in the isotherms behaviour should be pointed out. It is noticeable the differences in the collapse point, which is the phase change observed when the value of $d\pi/dA$ decreases. BNPTCD presents a collapse area of ca. 42 $Å^2$, being ca. 49 $Å^2$ in the case of PTCDIPr. The collapse pressure is ca. 44 mN/m for BNPTCD, meanwhile the PTCDIPr isotherm collapses at 47 mN/m. This insight suggests a larger stability of the PTCDIPr Langmuir film if

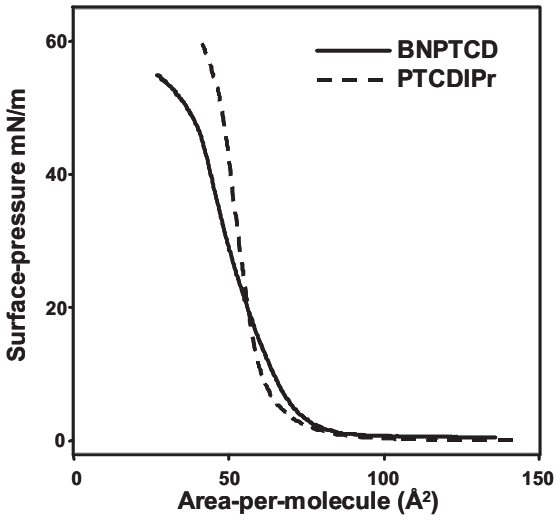

Fig. 2. Surface pressure–area isotherms of the BNPTCD (solid line) and PTCDIPr (dashed line) Langmuir films obtained at a water bath temperature of 20 °C.

compared to BNPTCD. Only at low surface pressures, the area per molecule is larger for BNPTCD than for PTCDIPr: 74 $Å^2$ for BNPTCD and 68 $Å^2$ for PTCDIPr at 4 mN/m. In other words, the PTCDIPr molecules start to feel the intermolecular interaction at the very first stage of the compression. However, the areas become identical (56 $Å^2$) at the beginning of the formation of the solid phases (ca. 18 mN/m). Beyond this point, the solid phase of the BNPTCD isotherm exhibit lower areas per molecule than that of PTCDIPr. It is also remarkable that the PTCDIPr isotherm shows a very stiff pressure rise. In contrast, the isotherm of BNPTCD presents a smoother behaviour during compression. All these observations correlate well with a larger coupling ability of the PTCDIPr molecules. Due to the reduced size of the bispropyl lateral chain, the perylene diimide moieties can get closer together in the case of PTCDIPr. In contrast, for the BNPTCD, the lateral neopentyl groups attached to the chromophore diminishes molecular stacking. The areas per molecule extrapolated to $\pi = 0$ for the Langmuir films are 70 and 61 $Å^2$ for BNPTCD and PTCDIPr. In view of the molecular size of the perylene and perylene diimides (see

Fig. 1) [15], the extracted areas-per-molecule at $\pi = 0$ require that the molecules for both derivatives organize with tilted head-on arrangement on the water subphase.

3.2. Electronic absorption spectra of solutions and thin LB films

Electronic absorption spectra of diluted solutions and 5-monolayer LB films for both perylene diimides are shown in Fig. 3. BNPTCD and PTCDIPr molecules show similar absorption profiles in CH_2Cl_2/TFA dilute solutions. The spectra consist in the characteristic vibronic structured absorption bands assigned to the π–π^* electronic transitions of PTCDs [17]. For BNPTCD the 0–0 transition band appears at 524 followed by the 0–1, 0–2 vibronic progressions at 488 and 456 nm. In the case of PTCDIPr the same vibronic pattern appears at 539, 501 and 468 nm, respectively. The fact that electronic absorption bands of the PTCDIPr are slightly shifted to higher wavelength values (15 nm that of 0–0 vibration) is in agreement with the lower optical gap value found for the PTCDIPr free molecule, 2.45 versus 2.49 eV for BNPTCD [18]. In the solid films, band broadening can be observed as a result of molecular packing. The PTCDIPr LB film absorption spectrum shows π–π^* electronic transition band with main components centred at 456, 556 and 612 nm. The absorption spectrum of the BNPTCD LB film exhibits a splitting of the π–π^* electronic transition band with one blue-shifted component, with peaks at 499 and 466 nm, and one red-shifted component, main peak at 543 nm with shoulder at 569 nm. For PTCDIPr, the thin film absorption spectrum appears considerably more red-shifted respect to the solution (73 nm) than that of the BNPTCD film (45 nm). In addition, the band broadening is more significant in the PTCDIPr LB film if compared to BNPTCD. Thus, in spite of the similar molecular structure, it can be concluded that PTCDIPr molecules show a larger tendency to dipole stacking and aggregation in solid films.

Fig. 4 shows the variation of peak absorbance at 499 nm for BNPTCD and 456 nm for PTCDIPr when increasing the number of transferred layers onto the substrate. A linear relationship is maintained up to 12th transferred monolayer for PTCDIPr, up to eighth for BNPTCD. This insight suggests that the deposition of the monolayers proceeded regularly at these levels. The linearity failed for further layer transferring, and consequently, the quality of the LB films beyond these limits is rather poor. These results concur with the transfer ratios obtained during LB film fabrication.

3.3. AFM measurements

Topographical AFM images of 5-monolayer and 15-monolayer LBs fabricated on cleaved mica were recorded to visualize the effect of increasing

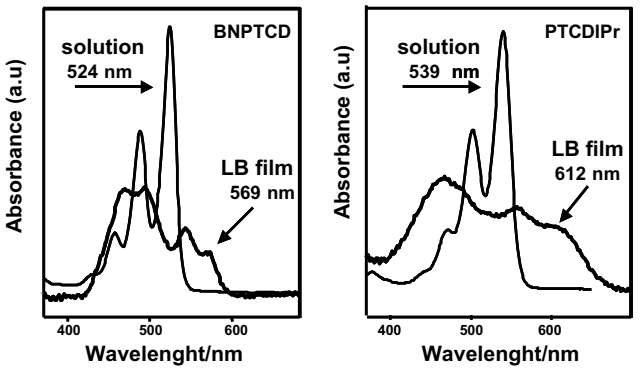

Fig. 3. Electronic absorption spectra of diluted solutions and 5-monolayers BNPTCD and PTCDIPr LB films. Arbitrary units are used allowing comparison.

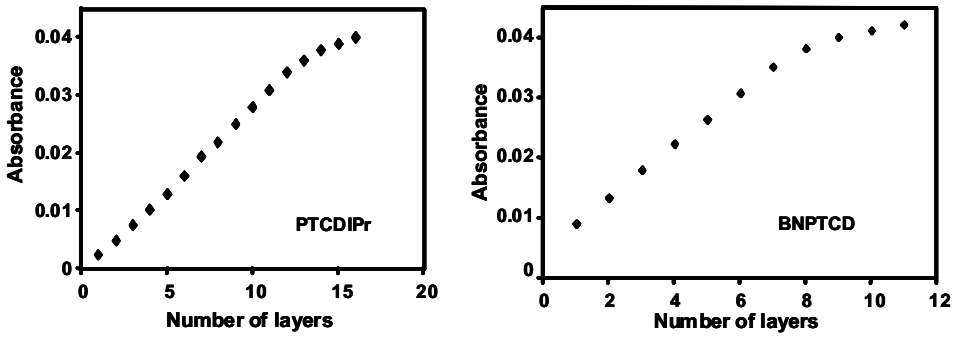

Fig. 4. Variation of peak absorbance, at 499 nm for BNPTCD, and 456 nm for PTCDIPr when increasing number of transferred monolayers.

the number of transferred layers on film morphology. As seen in Fig. 5(a), the 5-monolayer PTCDIPr LB film shows regular and overall homogeneous morphology with an estimated average roughness of 1.2 nm. However, the 2D micrograph of the 15-monolayer PTCDIPr LB film (Fig. 5(b)) shows the boost of porosity and roughness when the number of transferred monolayers is increased. The loosing of film quality and homogeneity is more significant in the case of BNPTCD (Fig. 5(c)–(f)). The morphology changes from homogeneous to sharply rough as the number of transferred monolayers is increased from 5 to 15. Moreover, the surface line profile hints that film growth takes place irregularly for the 15-monolayer BNPTCD LB film; pinholes and bulky granular structures are apparent (Fig. 5(f)). The AFM is consistent with the UV–Vis findings; within the linear variation of absorbance versus number of transferred monolayers homogenous LB films are obtained. Beyond this point, the film quality decreases drastically.

3.4. Molecular orientation in Langmuir–Blodgett films. RAIRS measurements

Polarization IR spectroscopy have been extensively used in the characterization of LB films since it allows one to determine the molecular orientation on surfaces [19–21]. The relative intensity of the vibrational modes in the spectrum can be explained in terms of the incoming infrared beam and the directionality of the dipole moments. Reflection–absorption infrared spectroscopy (RAIRS) profits from the perpendicular polarization of the electrical field at the nodal point on the reflecting surface plane. Therefore, the intensity of the vibrational modes with dynamic dipole components perpendicular to the surface will be enhanced, while those parallel to the surface will be suppressed as a consequence of 'the surface selection rule'. Pellet (bulk) transmission spectrum, where the material is dispersed in a KBr matrix, is used as reference. This system ensures a random spatial distribution of the active molecules dynamic dipoles. Thus, information about the molecular orientation can be extracted by comparing the KBr and RAIR spectra. The PTCDIPr vibrational IR spectrum can be summarized as follows: C–H wagging out-of-plane modes centred at 746, 810 an 850 cm^{-1}, two main C–H bending in-plane bending modes centred at 1077 and 1251 cm^{-1}, C–N in-plane stretching mode at 1343 cm^{-1}, C=C in-plane stretching mode at 1595 cm^{-1}, and C=O in-plane stretching symmetric and antisymmetric modes at 1662 and 1697 cm^{-1}, respectively. As seen in Fig. 6, almost a total suppression of the C–H wagging out-of-plane modes is observed in the RAIR spectrum of the 5-monolayer PTCDIPr LB film if compared to that of KBr. The RAIR spectrum also shows a decrease in the relative intensity of the C–H in-plane bending modes if compared to other in-plane modes. The C=O antisymmetry mode becomes prominent. These changes in relative intensities of the RAIRS, where the modes out of the chromophore plane are

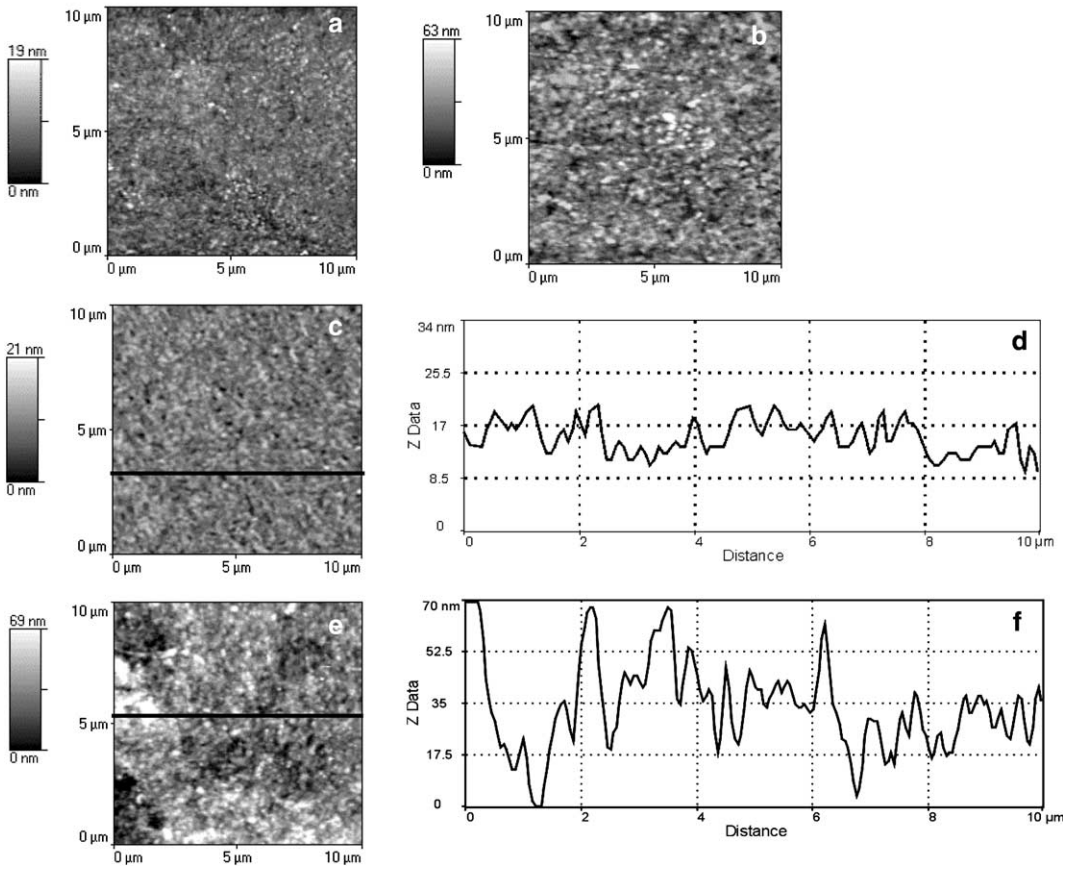

Fig. 5. AFM topographical image of (a) 5-monolayer and (b) 15-monolayer PTCDIPr LB films. (c) 2-D micrograph and (d) surface line profile of 5-monolayer BNPTCD LB film. (e) 2D micrograph and (f) surface line profile of 15-monolayer BNPTCD LB film.

suppressed and certain in-plane modes of the perylene moiety are enhanced, correlates with a preferential head-on orientation of the PTCDIPr molecules in the LB film. Similar conclusion can be extracted by comparison of the KBr spectrum and RAIRS of the 5-monolayer BNPTCD LB film (also shown in Fig. 6). The BNPTCD molecules are arranged with a head-on alignment over the substrate. The IR analysis evidences that the molecular organization found in Langmuir films is preserved when the monolayers are transferred onto substrates. Finally, It should be pointed out that the observed vibrational modes appear unshifted in the RAIR spectra with respect to the KBr spectrum. Then, no chemical bonding between the metal surface and any of the two species takes place.

3.5. Emission spectra

The BNPTCD and PTCDIPr 5-monolayer LB films emission spectra evidence the difference in molecular packing between derivatives (Fig. 7). The emission spectra were recorded using the 514.5 nm excitation source to excite mainly monomeric chromophore. The absorption spectra of concentrated solutions of perylene diimides usually exhibit a prominent dimer peak centred at wavelengths of ca. 600 nm [13]. Thus, the used of higher wavelength excitation sources might lead to the direct excitation of ground state dimers or higher aggregates found in the solid film. The spectrum of the PTCDIPr LB film consists in a broad featureless band with maximum centred at 657 nm, which can be assigned as an emission that

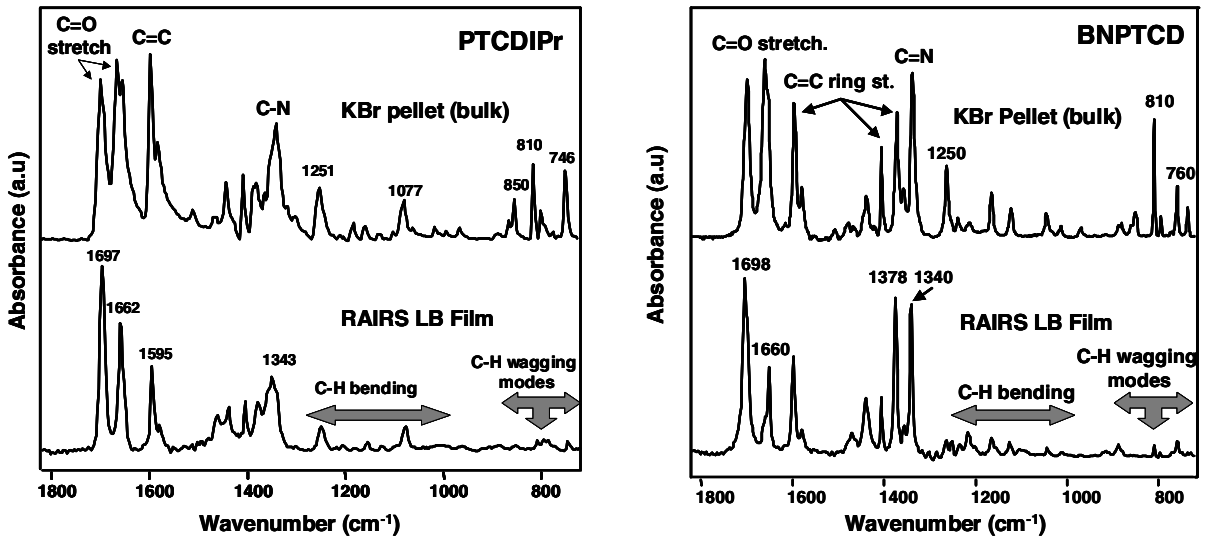

Fig. 6. Reflection–absorption infrared spectra (RAIRS) of 5-monolayers BNPTCD and PTCDIPr LB film. Transmission reference spectra (KBr pellet) are also shown for comparison.

of excimers [22]. This excimeric like luminescence is typically observed in perylene-based solid films, not only in bulk, but also at extremely low coverage ultra-thin films [7]. As reported by Schlettwein et al., excited dimer emissions become predominant in thin films of perylene derivatives thicker than two monolayers [6]. The PTCDIPr film excimeric spectral feature suggests that the interactions between adjacent molecules must be considerable, and need to be allowed by extended molecular coupling. The reduced size of the propyl alkyl chains permits the PTCDIPr chromophore to get crowded. On the other hand, the BNPTCD LB films spectrum shows a broad band (260 nm width) with two maxima at 590 and 642 nm, which correspond to a monomeric and excimeric like emissions, respectively. Although the excimer emission is significant, the monomeric feature, stronger in intensity, results to be the main excitation deactivation path. This evidence suggests a weaker interaction between adjacent BNPTCD moieties hinted by the sizes of the neopentyl groups attached. Moreover, the restrained molecular coupling in the BNPTCD film leads to a higher emission quantum-efficiency than in PTCDIPr. In this case, the emission quenching effect due to extended molecular packing is notable.

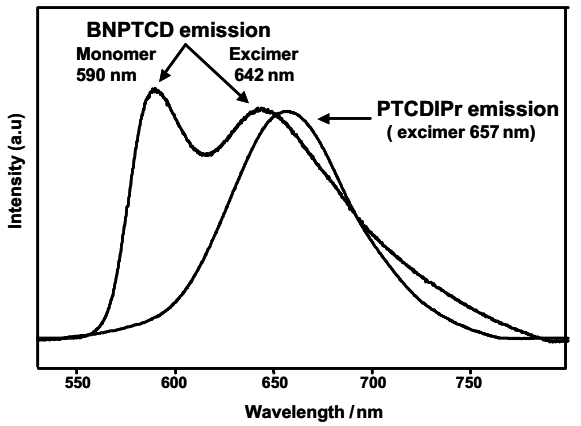

Fig. 7. Emission spectra obtained for 5-monolayers BNPTCD and PTCDIPr LB films using the 514.5 nm excitation source. Assigned monomer and excimer emission bands are marked.

4. Conclusions

Langmuir and Langmuir–Blodgett films of two different perylene derivatives have been fabricated and characterized. It has been found that good quality and ordered thin films can be obtained by means of this technique up to a certain number of transferred monolayers. As extracted from

Infrared data, the LB films of both dyes show preferential head-on molecular orientation over the substrate. Nevertheless, the PTCDIPr adjacent molecules show higher tendency to get coupled that leads to an excimeric like emission feature in solid thin films. In contrast, the neopentyl group attached to the perylene moiety in BNPTCD restricts intermolecular interaction favouring monomer emission over excimer.

Acknowledgements

Financial support from CICYT (Grant no. AGL2001-2104-C02-01) is gratefully acknowledged T.D.C. acknowledges a fellowship from the Spanish Ministry of Education (FPU Program). R. Aroca acknowledges financial assistance provided by the Spanish Ministry of Education, within the program '*Foreign Professors on sabbatical leave*' (*SAB2002-0017*).

References

[1] J.H. Burroughes, D.D.C. Bradley, A.R. Brown, R.N. Marks, K. Mackay, R.H. Friend, P.L. Burn, A.B. Holmes, Nature 347 (1990) 539.
[2] C.W. Tang, Applied Phys. Lett. 48 (1986) 183.
[3] I. Seguy, P. Jolinat, P. Destruel, J. Farenc, R. Mamy, H. Bock, J. Ip, T.P. Nguyen, J. Appl. Phys. 89 (2001) 5442.
[4] G. Horowitz, F. Kouki, P. Spearman, D. Fichou, C. Nogues, X. Pan, F. Garnier, Adv. Mater. 8 (1996) 242.
[5] S. Tasch, E.J.W. List, C. Hochfilzer, G. Leising, U. Rohr, P. Schlichting, Y. Geerst, A. Scherft, K. Müllen, Phys. Rev. B 56 (1997) 4479.
[6] D. Schlettwein, A. Back, B. Schilling, B. Fritz, N.R. Armstrong, Chem. Mater. 10 (1998) 60.
[7] E. Johnson, R. Aroca, Can. J. Chem. 91 (1991) 168.
[8] T. Del Cano, J. Duff, R. Aroca, Appl. Spectrosc. 56 (2002) 744.
[9] K.L. Lee, Y. Zu, A. Herrmann, Y. Geerts, K. Müllen, A.J. Bard, J. Am. Chem. Soc. 121 (1999) 3513.
[10] V. Shklover, F.S. Tautz, R. Scholz, S. Sloboshanin, M. Sokolowski, J.A. Schafefer, E. Umbach, Surf. Sci. 454–456 (2000) 60.
[11] P.A. Antunes, C.J.L. Constantino, R. Aroca, Langmuir 17 (2001) 2958.
[12] M.C. Petty, Langmuir–Blodgett Films. An Introduction, Cambridge University Press, Cambridge, 1996.
[13] P. Schouwink, A.H. Schäfer, C. Seidel, H. Fuchs, Thin Solid Films 372 (2000) 163–168.
[14] S. Rodriguez-Llorente, R. Aroca, J. Duff, J. Mater. Chem. 8 (1998) 2175.
[15] F.S. Tautz, S. Sloboshanin, J.A. Schafefer, R. Scholz, V. Shklover, M. Sokolowski, E. Umbach, Phys. Rev. B 61 (2000) 16933.
[16] A. Kam, R. Aroca, J. Duff, C.P. Tripp, Chem. Mater. 10 (1998) 172.
[17] M. Adachi, Y. Murata, S. Nakamura, J. Phys. Chem. 99 (1995) 14240.
[18] V. Parra, T. del Caño, M.L. Rodríguez-Méndez, J.A. de Saja, R.F. Aroca, Chem. Mater., accepted.
[19] J. Rabolt, F.C. Burns, N.E. Schlotter, J.D. Swalen, J. Chem. Phys. 78 (1983) 946.
[20] P.A. Chollet, J. Messier, C. Rosilio, J. Chem. Phys. 64 (1976) 1042.
[21] T. Del Cano, R. Aroca, J.A. De Saja, M.L. Rodriguez-Mendez, Langmuir 19 (2003) 3747.
[22] W.T. Yip, D.H. Levy, J. Phys. Chem. 100 (1996) 11539.